Received March 2004
Revised October 2004
Accepted February 2005

Combined radiative and convective heat transfer in a divided channel

H. Bouali and A. Mezrhab
Département de Physique, Faculté des Sciences, Universite Mohamed Premier, Oujda, Morocco

Abstract

Purpose – This paper presents a numerical investigation of the interaction of surfaces radiation with developing laminar free convective heat transfer in a divided vertical channel. The influence of the radiation on the heat transfer and on the air flow is studied for various sizes (width and length) of the plate.

Design/methodology/approach – The specifically developed numerical code is based on the utilization of the finite volume method. The SIMPLER algorithm for the pressure-velocity coupling is adopted. The view factors are determined by using boundary elements to fit the surfaces, an algorithm solving the shadow effect and a Monte Carlo method for the numerical integrations.

Findings – Results obtained show that the radiation: plays a very important role on the paces of the isotherms, especially at $Ra \geq 1{,}600$; increases considerably the average wall Nusselt number; and increases the mass flow rate and the average channel Nusselt number at high Rayleigh numbers. The plate location has a significant effect on the heat transfer only in presence of the radiation exchange. The increase of both length and width of the plate causes a decrease of the heat transfer and the mass flow rate.

Research limitations/implications – The use of the code is limited to the flow that is assumed to be incompressible, laminar and two dimensional. The radiative surfaces are assumed diffuse-gray.

Practical implications – Natural convection in vertical channels formed by parallel plates has received significant attention because of its interest and importance in industrial applications. Some applications are solar collectors, fire research, electronic cooling, aeronautics, chemical apparatus, building constructions, nuclear engineering, etc.

Originality/value – In comparison to the most of the previous studies on natural convection in partitioned channels, the radiation exchange was neglected. This study takes into account the radiation exchange in a divided channel.

Keywords Heat convection, Radiation, Channel flow

Paper type Research paper

Nomenclature

A = aspect ratio, $A = L/b$
A_i = radiative surface number i
b = channel width (m)
e = plate width (m)
g = gravity acceleration ($m\,s^{-2}$)
H_i = dimensionless incident radiation of surface A_i
K = thermal conductivity ($W\,m^{-1}\,K^{-1}$)
L = channel length (m)
L_i = distance of the plate from the channel inlet (m)
L_p = length of the plate (m)
Nu_c = average channel Nusselt number
Nu_w = average wall Nusselt number
N = total number of radiative surfaces
Nr = radiation number, $\sigma T_h^4/(k_f \Delta T/H)$
P = dimensionless pressure
p = pressure (Pa)

International Journal of Numerical Methods for Heat & Fluid Flow
Vol. 16 No. 1, 2006
pp. 84-106

0961-5539
DOI 10.1108/09615530610636973

Pr = Prandtl number, ν/α
Q = mass flow rate at the channel outlet ($m^2 s^{-1}$)
Ra = Rayleigh number, $g\beta(T_h - T_a)b^3/\nu\alpha$
Ra^* = channel Rayleigh number, Ra/A
R_i = dimensionless radiosity of surface A_i
R_k = thermal conductivity ratio, k_s/k_f
T = temperature (K)
T_a = temperature of the ambient air (K)
T_h = temperature of one hot wall (K)
T_o = average temperature, $(T_h + T_a)/2$ (K)
u, v = velocity component along x, y ($m s^{-1}$)
U, V = dimensionless velocity components along x, y
x, y = Cartesian coordinates (m)
X, Y = dimensionless Cartesian coordinates
α = thermal diffusivity ($m^2 s^{-1}$)
β = volumetric expansion coefficient (K^{-1})
ΔT = maximal difference temperature, $T_h - T_a$ (K)
$\Delta\theta$ = the step of isotherms
$\Delta\psi$ = the step of streamlines
ψ_{max} = maximal dimensionless stream function
φ_r = net radiative flux density ($W m^{-2}$)
ϕ_r = dimensionless net radiative flux density, $\varphi_r/\sigma T_h^4$
ν = kinematic viscosity of the fluid ($m^2 s^{-1}$)
ρ_o = density of the fluid at T_o ($Kg m^{-3}$)
Θ = dimensionless temperature, T/T_h
θ = dimensionless temperature, $(T - T_a)/(T_h - T_a)$
σ = Stefan-Boltzmann constant ($W m^{-2} K^{-4}$)
ε_i = emissivity of surface A_i

Subscripts
f = fluid
h = hot
s = solid
np = channel without plate
wp = divided channel

1. Introduction

Natural convection in vertical channels formed by parallel plates has received significant attention due to modern applications such as cooling of printed circuit boards, solar energy collectors, building construction and nuclear engineering. Elenbaas (1942) conducted the first experimental work, and proposed a correlation between the Nusselt number and the channel Rayleigh number. This work has served as a benchmark study for many numerical and experimental succeeding works. By examining a simplified set of equations, and by adjusting constants to fit experimental data, he established an overall heat transfer correlation for isothermal channel over a wide range of thermal and geometric parameters. The first numerical study of developing natural convective flow in an isothermal channel seems to be that of Bodoia and Osterle (1962). They used a boundary layer approximation, which gives good results for only the high Rayleigh numbers, because of the inlet boundary conditions chosen "Uniform velocity profile, ambient temperature and ambient pressure at the channel inlet". However, the overall heat transfer found in their study, was in good agreement with the experimental data of Elenbaas (1942). Aung *et al.* (1972) proposed a numerical and experimental investigation of the developing laminar free convection heat transfer in vertical parallel plate channels with symmetric and asymmetric heating. They considered two thermal boundary conditions of uniform wall temperature (UWT) and uniform wall heat fluxes (UHF). Numerical solutions are obtained for the developing flow and are shown to asymptotically approach the closed form solutions for fully developed flow. In the case of UWTs, the theoretical results were in concord with those obtained in experiments. Aihara (1973) has studied the effect of different inlet conditions for the parabolic problem and his prediction was found to agree with the correlation of the Nusselt number given by Elenbaas (1942). In fact, the boundary conditions at the entry of the channel were only approximate since

their determination for this kind of geometry is not obvious. Therefore, the parabolic equations are not precise since they are unaware of certain terms of the system controlling the thermal transfer and the airflow in the channel. Thus, the good agreement obtained between the numerical and experimental results was true because the selected cases were quite particular cases. Kettleborough (1972) and Nakamura *et al.* (1982) solved numerically the full elliptical model in this kind of configuration. Kettleborough has found a Nusselt number much higher than the one proposed by Elenbaas.

Natural convection in undivided channels was studied extensively by many authors, but the investigations concerning divided channels seem to be very few. Habchi and Acharia (1986) demonstrated that the ribs reduce the average Nusselt number of the divided channels, compared with the undivided ones. Naylor and Tarasuk (1993a) investigated numerically the natural convection in a divided vertical channel. The dividing plate was isothermal and has the same temperature of the channel walls. They analysed the effect of Rayleigh number and different parameters of the plate on the heat transfer rate from the channel walls, and presented the results of both the parabolic and elliptic solutions of the Navier-stokes and energy equations. They found that when the plate is positioning at the bottom of the channel, the average Nusselt number was maximum, and that the average Nusselt number of the dividing plate was two times much higher than that the one of the isolated plate. Tanda (1997) determined experimentally heat transfer data in vertical channels with one surface roughened by transverse square ribs. The results were compared with those obtained for undivided channels under the same geometries and boundary conditions. He concluded that the heat transfer performance of the divided channel turned out to be lower than that of the corresponding undivided channels. Thus, the ribs cause inactive regions near the upstream and downstream of each protrusion. Desrayaud and Fichera (2002) studied numerically the natural convection in a vertical channel obstructed by two symmetrical isothermal or adiabatic ribs. They found that the best position of the ribs for heat extraction depends on the magnitude of the Rayleigh number, and that the increase of the rib length has only a limited influence on the heat transfer while the increase of its width decreases dramatically the mass flow rate and the heat transfer especially when the region obstructed was greater than the half of the opening. More recently, a numerical investigation of the effect of circular and multiple rectangular wall block obstructions was achieved by Cruchaga and Celentano (2003). Their study was extended to higher Rayleigh numbers with respect to those previously reported in the literature. They concluded that, independently of the location or the geometries of the ribs, the average Nusselt number of the obstructed channels was lower than that of the undivided ones owing to the reduction of mass flow rate and the existence of stagnant regions caused by the obstructions. Andreozzi and Manca (2001) have studied the thermal and fluid dynamic behaviours of symmetrically heated vertical channels with auxiliary plate. They solved numerically the fully elliptic problem by a finite volume method for Rayleigh numbers and dimensionless plate height ranged between 10^3-10^6 and 0.0-1.0, respectively, and for a channel aspect ratio equal to 10. They proposed two correlations of the average Nusselt number, one for an adiabatic auxiliary plate and the other for a heated auxiliary plate. Andreozzi *et al.* (2002) conducted a numerical investigation of the influence of the fundamental thermo-geometrical parameters on natural convection heat transfer in vertical

channels with an auxiliary heated or adiabatic plate, correlations in a very simple form were proposed for specific ranges of *Ra*. The average Nusselt number was found to improve at high Rayleigh numbers for all the investigated configurations with the auxiliary plate with respect to the simple channel.

It seems that the studies of the obstructed channels were intensified in recent years, but the radiation exchange was neglected in the majority of these works. As a matter of fact, it is well known that when natural convection in air is involved, the heat transfer by convection and radiation are usually of the same order of magnitude. Combined radiative and convective heat transfer between vertical flat plates was first of all numerically investigated by Carpenter *et al.* (1976). It was found that at high Rayleigh numbers thermal radiation reduces considerably the heated wall temperature by keeping heat flux uniform and constant. Moutsoglou *et al.* (1992) conducted a numerical investigation of the natural convection heat transfer taking into account radiation in a vertical vented channel with uniform surface heat flux condition on the heated wall. It was found that for vented channels, the heated wall temperature increases above the corresponding unheated channel temperature throughout the region upstream of the farthest from the bottom vent location. It was concluded that, in general, vents deteriorate the overall cooling. Cheng and Müller (1998) investigated numerically the effect of heated wall temperature, the wall emissivity and the channel geometry on the turbulent natural convection coupled with thermal radiation in a vertical, rectangular channel with asymmetric heating. They concluded that even at low temperature of the heated wall, the high wall emissivity affected significantly the total heat transfer in the channel. In their study, a semi-empirical correlation was developed for the average Nusselt number. All these works have been restricted to the combined natural convection and thermal radiation heat transfer in the undivided channel.

The objective of this study is to investigate the radiation-natural convection interactions in a vertical divided channel heated symmetrically at uniform temperature. A complete parametric study is made for different Rayleigh numbers, emissivities of walls, locations of the plate in the channel, and sizes (length and width) of the plate.

2. Mathematical formulation

A schematic view of the problem, which consists of a divided vertical channel of width b, height L and aspect ratio $A = 5$, is shown in Figure 1. The plate is positioned in the vertical centerline of the channel.

The flow is assumed to be incompressible, laminar and two dimensional in a vertical divided channel. The walls are maintained at a temperature $T_h > T_a$. The working fluid is air and its physical properties are assumed to be constant at the average temperature T_o, except for the density whose variation with the temperature is allowed in the buoyancy term. The walls of the channel and the plate are assumed to be diffuse-gray surfaces. Then the dimensionless governing equations in the divided channel can be expressed as:

Continuity:

$$\frac{\partial U}{\partial X} + \frac{\partial V}{\partial Y} = 0 \tag{1}$$

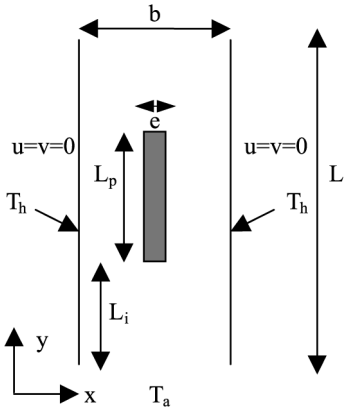

Figure 1.
Geometry of the divided channel

X momentum:

$$U\frac{\partial U}{\partial X}+V\frac{\partial U}{\partial Y}=-\frac{\partial P}{\partial X}+\lambda Pr\left(\frac{\partial^2 U}{\partial X^2}+\frac{\partial^2 U}{\partial Y^2}\right) \tag{2}$$

Y momentum:

$$U\frac{\partial V}{\partial X}+V\frac{\partial V}{\partial Y}=-\frac{\partial P}{\partial Y}+\lambda Pr\left(\frac{\partial^2 V}{\partial X^2}+\frac{\partial^2 V}{\partial Y^2}\right)+Ra\,Pr\,\theta \tag{3}$$

Energy:

$$U\frac{\partial \theta}{\partial X}+V\frac{\partial \theta}{\partial Y}=R_k\left(\frac{\partial^2 \theta}{\partial X^2}+\frac{\partial^2 \theta}{\partial Y^2}\right) \tag{4}$$

where λ, R_k are set equal to 1 in the fluid region and $\lambda=\infty$, $R_k=k_s/k_f$ in the solid region.

Referring to Figure 1, the dimensionless variables are the following:

$$X=x/b,\quad Y=y/b,\quad U=ub/\alpha,\quad V=vb/\alpha,\quad Pr=\nu/\alpha,$$

$$Ra=g\beta(T_h-T_a)b^3/\nu\alpha$$

$$P=(p+\rho_o gy)b^2/\rho_o\alpha^2,\quad Nr=\sigma T_h^4/(k_f\Delta T/b),\quad \theta=(T-T_a)/(T_h-T_a),$$

$$\phi_r=\varphi_r/\sigma T_h^4$$

A balance between radiation, conduction and convection determines the thermal condition at the surface of the plate:

$$R_k\frac{\partial \theta_s}{\partial n}=\frac{\partial \theta}{\partial n}-Nr\,\phi_r \tag{5}$$

where n denotes the unit normal direction to the surface at the solid-air interface and ϕ_r is the dimensionless net radiative flux density along this surface.

The governing equations were solved by a finite volume method under the following boundary conditions.

At the channel walls:

$$X = 0;1 \text{ and } 0 \le Y \le A: \quad U = V = 0, \quad \theta = 1, \quad \frac{\partial P}{\partial X} = 0 \tag{6}$$

At the inlet of the channel:

$$Y = 0 \text{ and } 0 \le X \le 1: \quad U = 0, \quad \frac{\partial V}{\partial Y} = 0, \quad \theta = 0, \quad P = -\frac{Q_i^2}{2} \tag{7}$$

At the outlet of the channel:

$$Y = A \text{ and } 0 \le X \le 1: \quad U = 0, \quad \frac{\partial V}{\partial Y} = 0, \quad \frac{\partial \theta}{\partial Y} = 0, \quad P = 0 \tag{8}$$

where Q_i is the mass flow rate at the channel inlet:

$$Q_i = \int_0^1 [V(X)]|_{Y=0} \, dX$$

For a sufficiently high channel Rayleigh numbers ($Ra^* \ge 100$), one can disregard the conduction effect upstream of the channel, and take the physical domain confounded with the one to simulate. The Bernoulli's equation is utilized for the pressure at the inlet of the channel.

To solve the equation (5), the radiation surface of the solid forming the channel and the solid plate are divided into a number of surfaces A_i, ($i = 1, N$). N is the number of total radiative surfaces forming the channel and the plate; which are equal to the total control volume interfaces solid-air. In fact, the control volume faces were also arranged so that a control volume face coincided with an interface solid-fluid. Therefore, the dimensionless net radiative flux density along a diffuse-gray and opaque surface A_i is expressed as:

$$\phi_{r,i} = R_i - H_i \tag{9}$$

where R_i and H_i are the dimensionless radiosity and incident radiation:

$$R_i = \varepsilon_i \Theta_i^4 + (1 - \varepsilon_i) H_i \tag{10}$$

The dimensionless radiative temperature Θ_i is given by:

$$\Theta_i = \frac{T_i}{T_h} = [(T_h - T_a)\theta_i + T_o]/T_h \tag{11}$$

For a divided channel consisting of N surfaces such that the radiative properties are uniform over each one of them, so we can express the radiation flux arriving at surface A_i by:

$$H_i = \sum_{j=1}^{N} R_j F_{i-j} \tag{12}$$

where F_{i-j} is the diffuse view factor between the two surfaces A_i and A_j.

The combination of equations (10) and (12) gives:

$$\sum_{j=1}^{N} (\delta_{ij} - (1 - \varepsilon_i) F_{i-j}) R_j = \varepsilon_i \Theta_i^4 \tag{13}$$

with δ_{ij} the Kronecker symbol.

The heat flux (q_w) at the side isothermal walls is the sum of the convective and radiative fluxes. In dimensionless form, the local heat flux is defined as follows:

$$\frac{q_w}{\left(k_f \frac{\Delta T}{b}\right)} = -\left.\frac{\partial \theta}{\partial X}\right|_{X_w, Y} + N_r \phi_r(X_w, Y) \tag{14}$$

where X_w is the position of the walls of the channel along the X-axis, i.e. $X_w \in \{0, 1\}$. Therefore, an overall local Nusselt number, based on the channel width, may be introduced such as:

$$Nu_w(X_w, Y) = Nu_{cv}(X_w, Y) + Nu_r(X_w, Y) \tag{15}$$

where Nu_{cv} and Nu_r are the convective and radiative contributions in Nu_w. The average Nusselt numbers, based on the channel width, along the side walls are determined by the integration of the expression (12) along the Y-axis:

$$Nu_w(X_w) = Nu_{cv}(X_w) + Nu_r(X_w) = \frac{1}{A} \int_0^A \left(-\left.\frac{\partial \theta}{\partial X}\right|_{X_w, Y} + N_r \phi_r(X_w, Y) \right) dY \tag{16}$$

Because of the perfect symmetry of the problem, we can write that: $Nu_w(0) = Nu_w(1)$. In this paper, the average wall Nusselt number ($Nu_w(0)$ or $Nu_w(1)$) is simply noted Nu_w.

In the same way, we defined the average channel Nusselt number Nu_c as follows:

$$Nu_c = \frac{1}{A} \int_0^1 [V(X)\theta(X)]|_{Y=A} \, dX \tag{17}$$

Finally, the mass flow rate at the outlet of the channel is defined as:

$$Q = \int_0^1 [V(X)]|_{Y=A} \, dX \tag{18}$$

3. Numerical procedure

Numerical solution of the governing differential equations was obtained by using a finite volume method, which utilizes a second-order central difference scheme (CDS) for the advective terms in order to reduce numerical diffusion errors. In the range of Rayleigh numbers investigated, the CDS solution did not exhibit spurious

oscillations and the convergence was achieved by using small under-relaxation factors on U, V and θ. The SIMPLER algorithm assures the pressure-velocity coupling. The governing equations were cast in transient form and a fully implicit transient differencing scheme was employed as an iterative procedure to reach steady state. The presence of the plate was accounted by the strategy in which a region of high viscosity characterizes it.

The resulting systems of discretized equations were solved by an iterative procedure based on a preconditioned conjugate gradient method. The outer iterative loop is repeated until the steady state is achieved. It is obtained when the following convergences are simultaneously satisfied: max $|\phi^{(n+1)} - \phi^{(n)}| < \varepsilon_\phi$ where ϕ is a dependant variable and n the iteration number (i.e. false time step). In most of the cases, the velocity components and temperature were driven to $\varepsilon_u = \varepsilon_v = \varepsilon_\theta < 10^{-6}$. For the pressure correction equation, which is a discretized Poisson equation, the iterative process was stopped when the maximum residual of mass (amount by which the continuity equation was not satisfied) was less than 10^{-8}.

For the combined radiation and convection problem, the surface temperatures on the plate were calculated from the non-linear heat balance equation (equation (5)) by using an inner iterative procedure at every time step for the energy equations. The grid was extended across the plate's boundaries by introducing one extra point in order to discretize equation (5). The surface temperatures were updated from the solution of the energy equation by under-relaxing the boundary evaluation of temperature. At each inner iteration, the linear system of equations for the radiosities (equation (13)) was solved by a direct method (Gauss elimination).

The grid was constructed such that the boundaries of physical domain coincide with the velocity grid lines. The points for pressure and temperature were placed at the center of the scalar volumes. At the fluid-plate interfaces, the control volume faces were also arranged so that a control volume face coincided with an interface. This grid distribution was chosen to ensure the interface energy balance. To avoid a check-board pressure and velocity fields, staggered grids were used for the U and V-velocity components in the X- and Y-directions, respectively.

Since the radiative properties of the solid surfaces of the plate vary from point (even on the isothermal side walls because the inside radiation cannot be assumed as uniform), each of the surfaces was divided into finite number of zones on which the four basic assumptions of the simplified zone analysis was assumed valid. The mesh used to solve the differential equations determined the number of zones retained. Therefore, the zoning was not uniform and the area of each zone varied according to the stretching function and number of grid points used. For N control volume faces, this results in $N(N-1)/2$ view factors to be calculated and in a linear system of N equations for the radiosities. The view factors were determined by using a boundary element approximation to fit the surfaces and on a Monte Carlo method for the numerical integrations (Mezrhab and Bchir, 1999).

We first varied the grid to determine the optimum non-uniform grid (i.e. the best compromise between accuracy and computational costs). In this study, a 30×102 grid points was chosen to optimise the relation between the accuracy required and the computing time (Table I). The grid is non-uniform and fine near the solid surfaces and tips of the plate.

4. Code validation

The code was extensively exercised on benchmark problems to check its validity. Computations were first performed for the classical problems of natural convection in the undivided channel. In this section, a comparison of our results with those reported by Naylor *et al.* (1991), Kettleborough (1972) and Nakamura *et al.* (1982) for natural convection in an undivided vertical channel, of an aspect ratio equal to 5, is presented for $Ra^* = 1,466$ and $Pr = 0.733$. Next, natural convection heat transfer in a divided vertical channel was considered. The solutions obtained for a divided vertical channel are compared with those of Naylor and Tarasuk (1993a, b).

Table II shows a comparison between our results and those obtained in Naylor *et al.* (1991), Kettleborough (1972) and Nakamura *et al.* (1982) for three quantities selected in Naylor *et al.* (1991): the average wall Nusselt number Nu_{m1}, the average channel Nusselt number Nu_{m2} and the mass flow rate Q_e. It should be noted that the relationship between the quantities (Nu_w, Nu_c and Q) defined in this paper and (Nu_{m1}, Nu_{m2} and Q_e) are as follows:

$$Nu_{m1} = \frac{Nu_w}{2}, \quad Nu_{m2} = \frac{Nu_c}{4} \text{ and } Q_e = Q\sqrt{\frac{2}{Ra\,Pr}}$$

As can be seen in Table II, all the quantities are in very good agreement for the case of an isothermal undivided channel.

In the case of a divided channel, comparisons of local and average wall Nusselt numbers, mass flow rates, and average channel Nusselt number were made with those given numerically and experimentally by Naylor and Tarasuk (1993a, b). In all cases, the present calculations gave identical results. For example of this validation, we present in Table III, the average wall Nusselt number, Nu_w and the plate Nusselt number, Nu_p obtained by our code and those of Naylor and Tarasuk (1993b) shown in Table I (p. 391).

When the radiation exchange is taken into account, the code was validated by studying the same problem and by taking the same values for the parameters as are

Table I.
Grid sensitivity test for $Ra^* = 1.6 \times 10^4$, $Pr = 0.71$, $e = 0.2\ b$, $A = 5$, $L_i = L/3$ and $L_p = L/3$

	20 × 90	30 × 90	30 × 102	30 × 120	40 × 120
Nu_c	12.228	12.508	12.516	12.525	12.520
Nu_w	6.186	6.370	6.368	6.367	6.363
Q	129.640	132.570	132.740	133.010	132.780
$\lvert\psi_{max}\rvert$	121.542	124.286	124.440	124.701	125.062

Table II.
Comparison of the average convective Nusselt numbers and the mass flow rate for $Ra^* = 1{,}466$, $Pr = 0.733$, $A = 5$

	Naylor *et al.* (1991)	Kettleborough (1972)	Nakamura *et al.* (1982)	Our results
Nu_{m1}	1.802	2.750	1.814	1.799
Nu_{m2}	1.867	2.380	1.877	1.870
Q_e	1.439	2.079	1.358	1.425

used in Moutsoglou *et al.* (1992). We obtain the same flow and temperature profiles. Concerning the average wall Nusselt number and the mass flow rate, the largest discrepancies between our results and those obtained by Moutsoglou *et al.* (1992) are less than 3 per cent.

Based on the above studies, it was concluded that the code could be reliably applied to the problem under consideration.

5. Results and discussion

The mathematical model developed in the last section was used to investigate the mutual interaction radiation-natural convection. Each case required the specification of eight dimensionless parameters (Ra, Pr, R_k, A, e, L_i, L_p, ε) among which the Prandtl number, the thermal conductivity ratio and the channel aspect ratio were held fixed at $Pr = 0.71$, $R_k = 1$ and $A = 5$. The remaining parameters have been varied with the aim of studying their effects on the heat transfer and the air flow in the channel. We suppose that all radiative surfaces have the same emissivity. The average temperature T_o is chosen equal to 300 K, and in order to keep available the Boussinesq approximation ($\Delta T < 0.1\, T_h$) (Zhong *et al.*, 1985), the terminal temperature difference ΔT is kept equal to 27 K. Hence, T_h and T_a will be, respectively, equal to 313.5 and 286.5 K.

When one holds into account the radiation exchange, the characteristic dimension of the channel (b) may be calculated for a specific Rayleigh number. Substituting the value of (b) into the expression of Nr gives:

$$Nr = \frac{\sigma T_h^4}{k\Delta T}\left(\frac{A\nu\alpha}{g\beta\Delta T}\right)^{\frac{1}{3}} Ra^{*1/3} \tag{19}$$

5.1 Effects of the surface emissivity

Figure 2 shows isotherms and streamlines for $160 \leq Ra^* \leq 16,000$ and ($L_i = L/3$, $L_p = L/3$ and $e = 0.2\ b$) in absence ($\varepsilon = 0$) and in presence ($\varepsilon \neq 0$) of the radiation exchange. The surface emissivity (ε) studied, was chosen equal to 0.25, 0.50, 0.75 and 1. Independently, of the value of ε, the isotherms are perfectly symmetrical with respect to the vertical line crossing the middle of the plate. The surface temperatures of the plate increase with the increasing of the surface emissivity and reach their maximum at $\varepsilon = 1$. For this value, the temperature gradients near the surface of the plate give an indication of the importance of the radiative flux, especially at high channel Rayleigh numbers ($Ra^* \geq 1{,}600$).

From the isotherms, it appears that the radiation exchange produces a good homogenization of surface temperatures in every region delimited by the isothermal

	Experiment results (Naylor and Tarasuk, 1993b)	Numerical results (Naylor and Tarasuk, 1993a)	Our results
Wall Nusselt number, Nu_w	1.44	1.60	1.57
Plate Nusselt number, Nu_p	3.13	3.48	3.41

Note: Comparison of the average Nusselt numbers at the wall and the plate for $Ra^* = 1561.6$, $Pr = 0.733$, $L_i = 0$, $e = 0.2\ b$, $A = 6.84$, $L_p = L/3$

Table III.

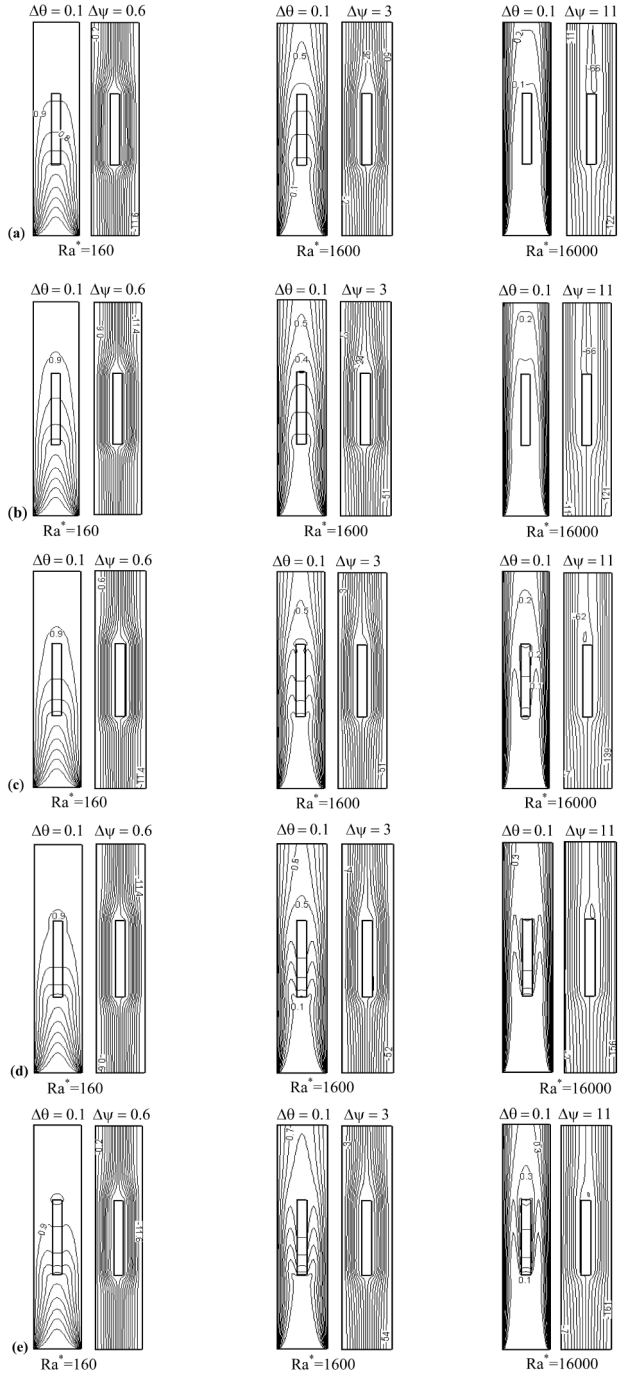

Figure 2.
Isotherms and streamlines: (a) $\varepsilon = 0$, (b) $\varepsilon = 0.25$, (c) $\varepsilon = 0.5$, (d) $\varepsilon = 0.75$ and (e) $\varepsilon = 1$

walls of the channel and the vertical boundaries of the plate. This is because the surface temperatures of the plate increase under the effect of radiative heat flux coming from the isothermal walls of the channel. Thus, the air temperature increases at the neighbourhood of the plate, which generates two small channels delimited by the isothermal walls and the vertical surfaces of the plate. We notice that the radiation effect is more pronounced at high channel Rayleigh numbers Ra^* because the radiation number Nr is proportional to Ra^* as indicated in equation (19), and increases with increasing Ra^*. The structures of the isotherms near the plate in presence of the radiation exchange indicate that the heat is transferred from the plate to the neighbouring fluid. However, in absence of the radiation exchange, the heat is transferred from the fluid to the plate.

The streamlines are also perfectly symmetrical across the vertical centreline. Furthermore, the radiation exchange increases the air velocity in the channel, particularly at high Ra^*.

Figure 3(a) shows the average wall Nusselt number (Nu_w) as a function of the channel Rayleigh number Ra^*. Independently of the value of ε, Nu_w increases with increasing Ra^*. Indeed, the increase of Ra^* yields an increase in both the buoyancy forces and the radiation number Nr, which allows the contributions radiative (Nu_r) and convective (Nu_{cv}) in Nu_w (equation (16)) to increase. For a constant Ra^*, Nu_w increases with increasing the surface emissivity ε. This is expected because the dimensionless net radiative flux density (ϕ_r) (which is counted in Nu_r) lost by a hot wall of the channel increases as a function of the surface emissivity ε. The radiation effect on Nu_c and Q is

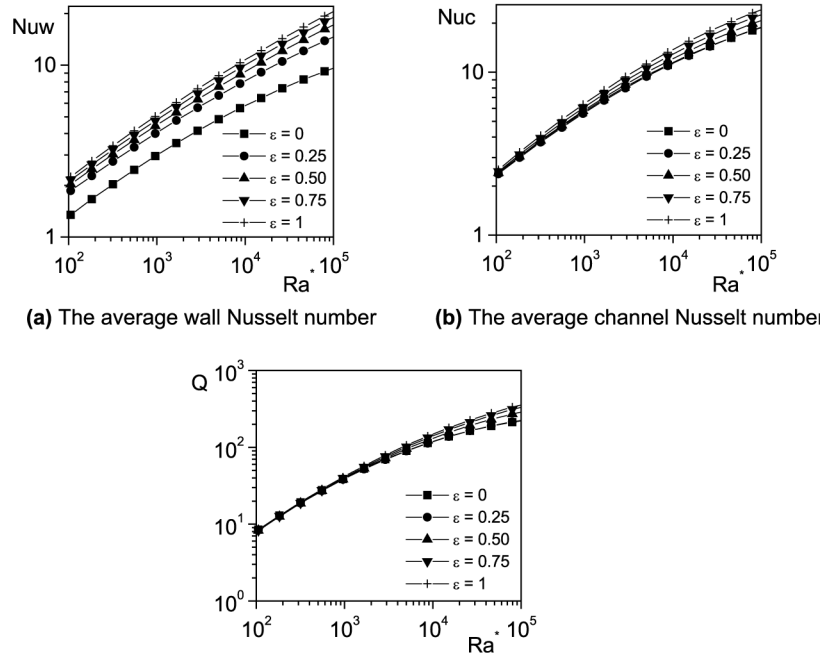

(a) The average wall Nusselt number

(b) The average channel Nusselt number

(c) The mass flow rate for $L_i = L/3$, $L_p = L/3$ and $\varepsilon = 0.2$b

Figure 3.
Effect of the surface emissivity

presented, respectively, in Figure 3(b) and (c). At moderates Ra^* ($Ra^* \leq 160$), the effect of the radiation exchange is negligible (Nr is small); whereas for ($Ra^* \geq 1{,}600$), we can observe that the radiation exchange increases both Nu_c and Q. This increase is especially important when Ra^* is elevated. In fact, at high Ra^*, the two small channels, generated under the radiation effect, contribute in a meaningful way to the increase of the mass flow rate through the outlet of the channel. Consequently, the average channel Nusselt number Nu_c and the mass flow rate Q increase.

5.2 Effects of the plate location

Figure 4 shows isotherms and streamlines for a channel Rayleigh numbers Ra^* ranging from 160 to 16,000 in presence (b and d) and in absence (a and c) of the radiation exchange for two positions (inlet and outlet) of the plate. When the plate is located at the center of the channel, the isotherms and streamlines are shown in Figures 2(a) ($\varepsilon = 0$) and Figure 2(e) ($\varepsilon = 1$). For a comparison purpose, the isotherms and streamlines for the undivided channel are also shown (for the same geometry and the same boundary conditions) in Figure 4(e) for $\varepsilon = 0$ or 1. Indeed, the radiation exchange has no effect on the heat transfer and the flow in the undivided channel because the channel walls are maintained at the same uniform temperature.

In the pure natural convection case ($\varepsilon = 0$), the air circulation is almost the same for the three locations of the plate; whereas it increases with moving the plate to the inlet in presence of the radiation exchange. When the plate is located near the inlet, the air (entering with the ambient temperature) is preheated due to the obstacle. Hence, the air temperature in this region (the inlet) is slightly elevated, particularly in presence of the radiation exchange with respect to the case where the plate is located near to the outlet. Indeed, the temperature of the plate increases under the radiation exchange (compared to the pure natural convection case) owing to the radiation emitted by the isothermal walls. Thus, the air, in the inlet region, is heated by both the isothermal walls and the vertical surfaces of the plate; whereas, in the pure natural convection case, the air is heated only by the isothermal walls. In all cases (inlet, center, outlet), the air temperature is greater than the one calculated in the undivided channel. This is due to the obstacle that reduces the air velocity, which allows the air to be heated more efficiently.

We report in Figure 5 the effect of the plate location on Nu_w, Nu_c and Q in the pure natural convection case. It is clear that the location of the plate has no significant effect on these three numbers characterizing the heat transfer and fluid flow in the channel. However, they are smaller than those of the undivided channel, particularly at low Ra^* ($Ra^* \leq 1{,}600$). This is because the quantity of the fluid in the undivided channel is more important than the one in the divided channel (the space occupied by the plate reduces the total quantity of the flow in the channel). Therefore, the total heat absorbed by the fluid is more important. In addition, at low Ra^*, the flow is fully developed (the dimensionless temperature at the outlet is almost equal to 1), and since the air velocity is reduced by the obstruction, then Nu_c and Q are significantly reduced, compared with those obtained for the undivided channel.

In presence of the radiation exchange (Figure 6), Nu_w, Nu_c and Q increase slightly with moving the plate from the outlet to the inlet of the channel. The average wall Nusselt number Nu_w, for the three location of the plate, is greater than that of the

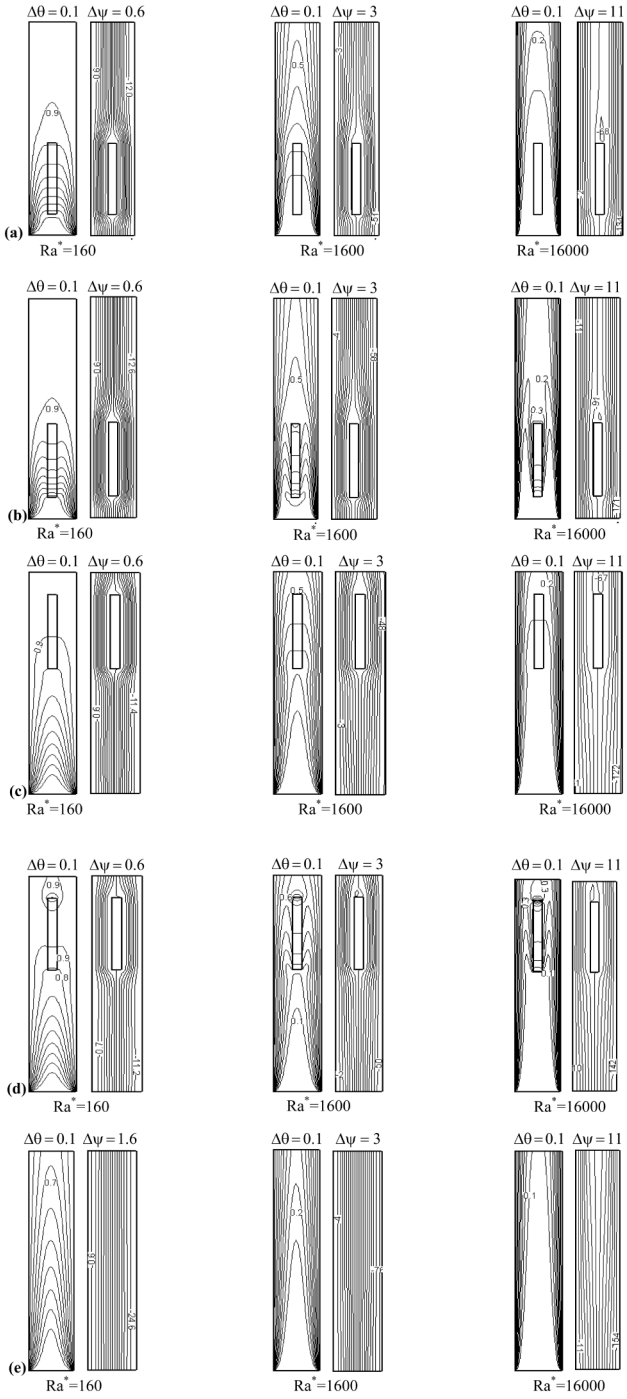

Figure 4.
Isotherms and streamlines for $L_p = L/3$ and $e = 0.2\ b$: (a) $\varepsilon = 0$, $L_i = 0.1\ L$, (b) $\varepsilon = 1$, $L_i = 0.1\ L$, (c) $\varepsilon = 0$, $L_i = 0.9\ L - L_p$, (d) $\varepsilon = 1$, $L_i = 0.9\ L - L_p$ and (e) undivided channel $\varepsilon = 0$ or 1

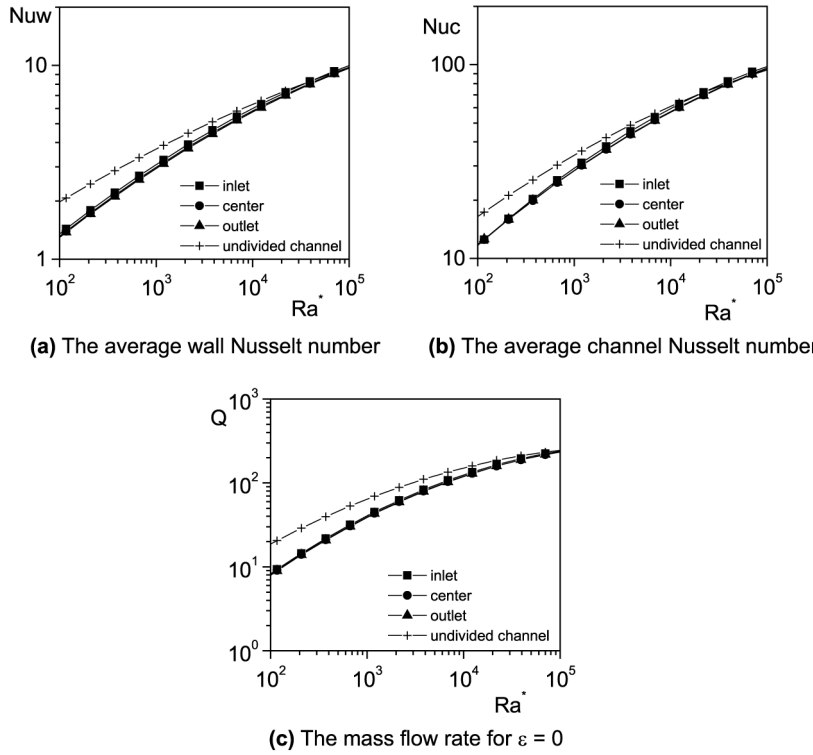

Figure 5.
Effect of the location of the plate

undivided channel, especially at high Ra^* (to which corresponds a high radiation number Nr) (Figure 6(a)). As a matter of fact, the effect of the radiation exchange is negligible in the case of the undivided channel. This is due to the fact that both walls of the channel are maintained at the same temperature. On the other hand, the average Nusselt number of the divided channel, $Nu_{c_{wp}}$, is lower than that of the undivided channel, $Nu_{c_{np}}$, until $Ra^* = 1{,}700$, when the plate is located near the channel inlet. $Nu_{c_{np}}$ becomes equal to $Nu_{c_{wp}}$ at $Ra^* = 3{,}000$, when the plate is located at the center, and at $Ra^* = 5{,}000$ when it is located near the outlet of the channel (let us recall that this last position reduces the average Nusselt numbers). Beyond $Ra^* = 5{,}000$, $Nu_{c_{np}}$ becomes lower than $Nu_{c_{wp}}$ for any location of the plate and the difference between $Nu_{c_{np}}$ and $Nu_{c_{wp}}$ increases with increasing Ra^* (Figure 6(b)). The effect of the radiation exchange on the mass flow rate is negligible until $Ra^* = 9{,}600$ (Figure 6(c)). Beyond this value, the mass flow rate for the divided channel becomes important in comparison with that of the undivided channel. Indeed, even if the plate obstructs the flow, the radiation exchange, that becomes important at high Ra^*, contributes in a meaningful way to the increase of the mass flow rate by the creation of two small channels.

5.3 Effects of the plate length

Figure 7 shows streamlines and isotherms for two extreme values of the plate length ($L_p = 0.1\ L$ and $L_p = 0.8\ L$). In both cases ($\varepsilon = 0$ and $\varepsilon = 1$), we note that the air

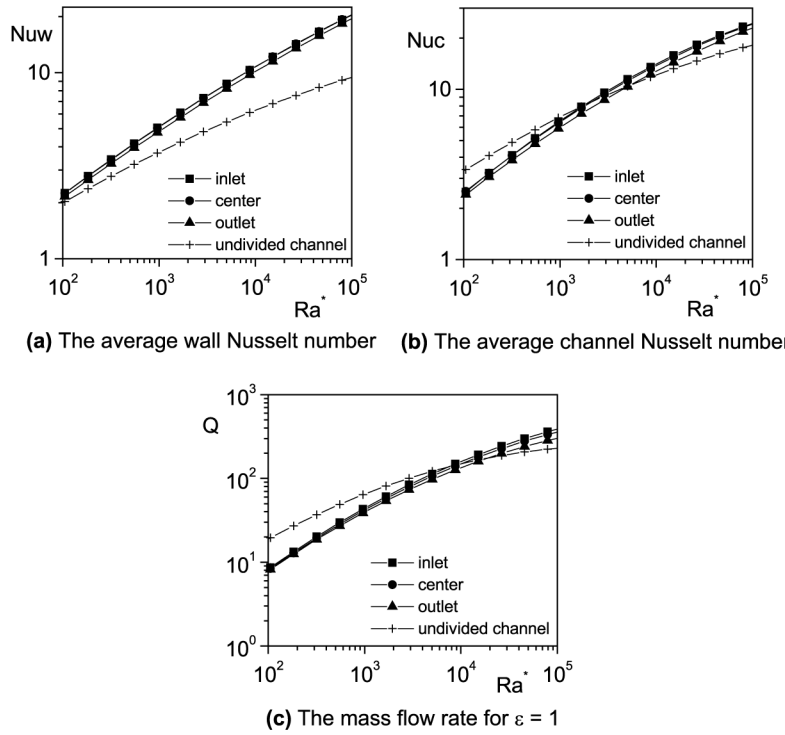

Figure 6.
Effect of the location of the plate

velocity in the channel decreases with increasing the plate length, particularly when $Ra^* = 160$. This is expected due to the presence of the plate which obstructs the flow and also to the weak value of Nr which corresponds to $Ra^* = 160$. As can be seen, for $L_p = 0.8\,L$, $\varepsilon = 0$ and $Ra^* = 16{,}000$, the air velocity decreases (with respect to the case of $L_p = 0.1\,L$), so there will be less cold air that enters the channel; which explains the increase of the air temperature inside the channel. Contrarily to the pure natural convection case, the increase of the plate length causes an increase of the air velocity when $Ra^* = 16{,}000$ and $\varepsilon = 1$. This is due to the increase of the surface temperatures of the plate under the effect of the radiative heat fluxes coming from the two heated walls of the channel. Hence, two channels delimited by the plate's vertical boundaries and the walls of the channel are generated; which explains the structure of isotherms (at $Ra^* = 16{,}000$ and $\varepsilon = 1$). We notice that the radiation exchange has no significant effect when the plate's length is small ($L_p = 0.1\,L$); whereas, it strongly affects the isotherms and streamlines when the plate's length is large ($L_p = 0.8\,L$). It is evident because the number of radiative surfaces of the plate increase with increasing L_p and, of this fact, the radiative heat fluxes captured by the vertical surfaces of the plate become important.

Figure 8(a) shows, in the absence of the radiation exchange ($\varepsilon = 0$), Nu_w for three different lengths (L_p) of a plate of fixed width ($e = 0.2\,b$) and located at $L_i = 0.1\,L$ from the channel inlet. Let us note that the increase of the plate length causes a decrease of Nu_w until $Ra^* = 40{,}000$ and, beyond this value, the effect of the plate length is reversed

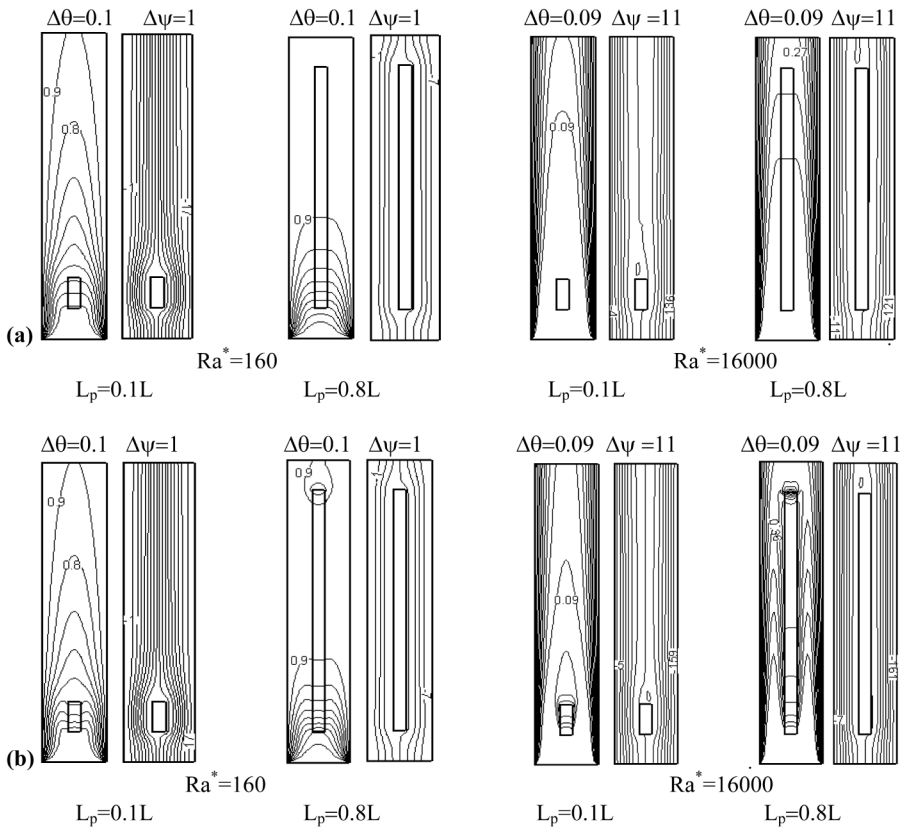

Figure 7.
Isotherms and streamlines for $L_i = 0.1\ L$ and $e = 0.2$ *b*: (a) $\varepsilon = 0$, (b) $\varepsilon = 1$

and $Nu_{w_{np}}$ becomes lower than $Nu_{w_{wp}}$ for all the plate lengths. Indeed, at low values of Ra^*, the increase of the plate length reduces the air velocity, whereas the flow is developed (the temperature of the field reaches its maximum before the exit), and consequently Nu_w is proportional to the flow velocity like the one which is demonstrated by Teertstra *et al.* (1995). Hence, Nu_w decreases with decreasing the air velocity. However, at high Ra^* ($Ra^* > 40{,}000$), the buoyancy forces become elevated and although the increase of the plate length yields a decrease in the air velocity, it produces, on the other hand, an increase of the local air temperature.

The same explanation is valid for the plate length effect on Nu_c and Q (Figure 8(b) and (c)).

The radiation exchange increases $Nu_{w_{wp}}$ and $Nu_{c_{wp}}$ for the three values of the plate length, especially at high Ra^* (Figure 9(a) and (b)). However, $Nu_{w_{wp}}$ (respectively, $Nu_{c_{wp}}$) corresponding to the highest $L_p = 0.8\ L$ remains lower than $Nu_{w_{np}}$ (respectively, $Nu_{c_{np}}$) until $Ra^* = 300$ (respectively, $Ra^* = 4{,}000$). It is also seen that until $Ra^* = 4{,}000$, the value of $Nu_{w_{wp}}$ (respectively, $Nu_{c_{wp}}$) is almost the same for $L_p = L/10$ and $L_p = L/3$; but it is superior to the one corresponding to $L_p = 0.8\ L$. When $4{,}000 \leq Ra^* \leq 40{,}000$, the effect of the plate length is almost negligible on

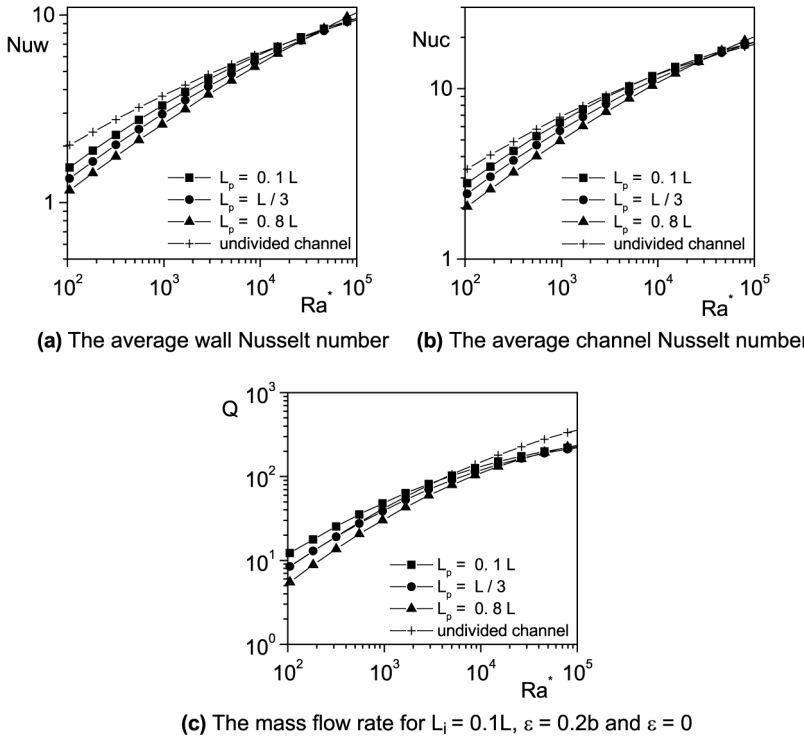

(a) The average wall Nusselt number **(b)** The average channel Nusselt number

(c) The mass flow rate for L_i = 0.1L, ε = 0.2b and ε = 0

Figure 8.
Effect of the plate length

$Nu_{w_{wp}}$ and $Nu_{c_{wp}}$. However, when Ra^* exceeds 40,000, the tendency is reversed and the heat transfer increases with the increasing of the plate length.

The mass flow rate at the outlet of the channel is less affected by the radiation exchange (Figure 9(c)), and the value of Ra^* at which Q_{np} becomes equal to Q_{wp} is $Ra^* = 8{,}000$. Let us note that until this value of Ra^*, the plate length plays an important role in the reduction of the flow. Beyond $Ra^* = 10^4$, Q_{np} becomes lower than Q_{wp} and the mass flow rate is especially important when the length of the plate is large. In fact, at $Ra^* \geq 10^4$, the surface temperatures of the plate increase under the effect of radiation (*Nr* is important); therefore, more of the air is aspired because of the effects of the two channels (created under the effects of radiation).

In summary, the effect of the plate length on Nu_w, Nu_c and Q, in presence of the radiation exchange ($\varepsilon = 1$), is similar to the one observed in the pure natural convection case ($\varepsilon = 0$) but with a difference in the values of Ra^* at which this effect is reversed.

5.4 Effect of the plate width

As can be seen in Figure 10, the radiation exchange does not have any considerable effect on the isotherms and streamlines for $Ra^* = 160$, whereas it affects them strongly for $Ra^* = 16{,}000$. This is expected owing to the radiation number *Nr* which is higher at $Ra^* = 16{,}000$ and lower at $Ra^* = 160$. The apparition of two small channels,

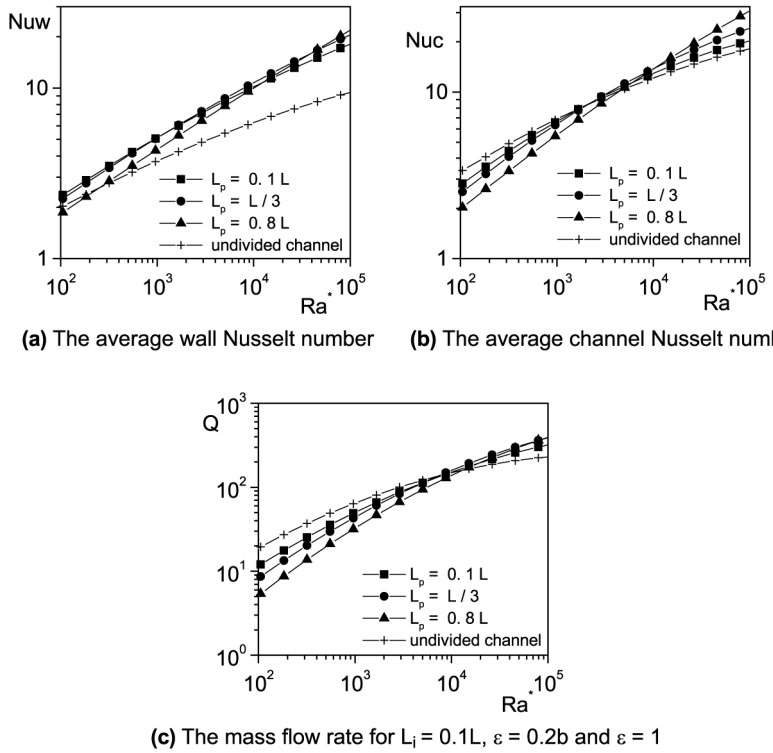

Figure 9.
Effect of the plate length

between the plate's vertical boundaries and the channel walls (at $\varepsilon = 1$), is due to the increase of the plate's temperature under the influence of the radiative heat flux coming from the channel walls. This is the chimney effect, which increases considerably the velocity of the field. For both cases ($\varepsilon = 0$ and $\varepsilon = 1$), the increase of the plate's width causes a decrease in the air circulation.

For a constant length of the plate located at $L_i = L/3$, Figure 11 shows the effect of the plate's width on Nu_w, Nu_c and Q in the pure natural convection case ($\varepsilon = 0$). The figure shows that, for $Ra^* \leq 40{,}000$, Nu_w and Nu_c decrease with the increasing of the plate width. Beyond this value of Ra^*, the effect of the plate length is reversed. It is due to the decrease of the total air mass in the channel, and we have the same explanation given for Figures 8 and 9 concerning the effect of the plate length. At low Ra^* the regime is developed. Thus, the air velocity is maximum in the centre part of the undivided channel; however, it is strongly reduced in presence of the plate, which explains the very important decrease in the mass flow rate through the outlet of the channel for the divided channels.

Once again, it is shown in Figure 12(a) that the radiation exchange increases considerably Nu_w. It also reduces the gaps observed, in the pure natural convection case, between the average Nusselt numbers Nu_w corresponding to the three plates. However, the effect of the radiation exchange on Nu_c (Figure 12(b)) and Q (Figure 12(c))

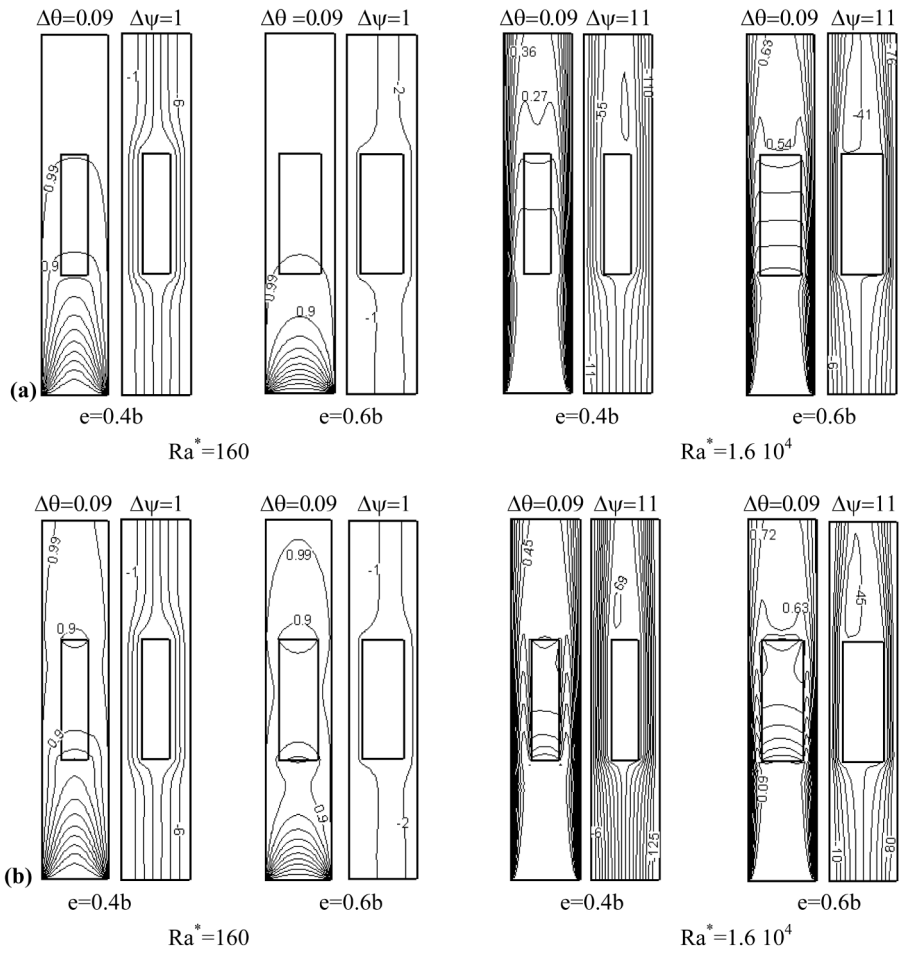

Figure 10.
Isotherms and streamlines for $L_i = L/3$ and $L_p = L/3$: (a) $\varepsilon = 0$, (b) $\varepsilon = 1$

is also not important. On the other hand, the effect of the plate width in presence of radiation exchange ($\varepsilon = 1$) on Nu_w, Nu_c and Q is similar to the one observed in the pure natural convection case ($\varepsilon = 0$); but with a difference in the values of the channel Rayleigh numbers Ra^* at which this effect is reversed.

6. Conclusion

A numerical study of the combined natural convection with radiation heat transfer in a divided channel has been presented. A good agreement was obtained with the references, concerning obstructed and unobstructed channels. The effects of radiation exchange, emissivities of solid surfaces, locations and sizes (length and width) of the plate have been analysed. The results were presented in terms of isotherms and streamlines patterns, the average wall Nusselt number (Nu_w), the average channel Nusselt number (Nu_c) and the mass flow rate at the outlet of the

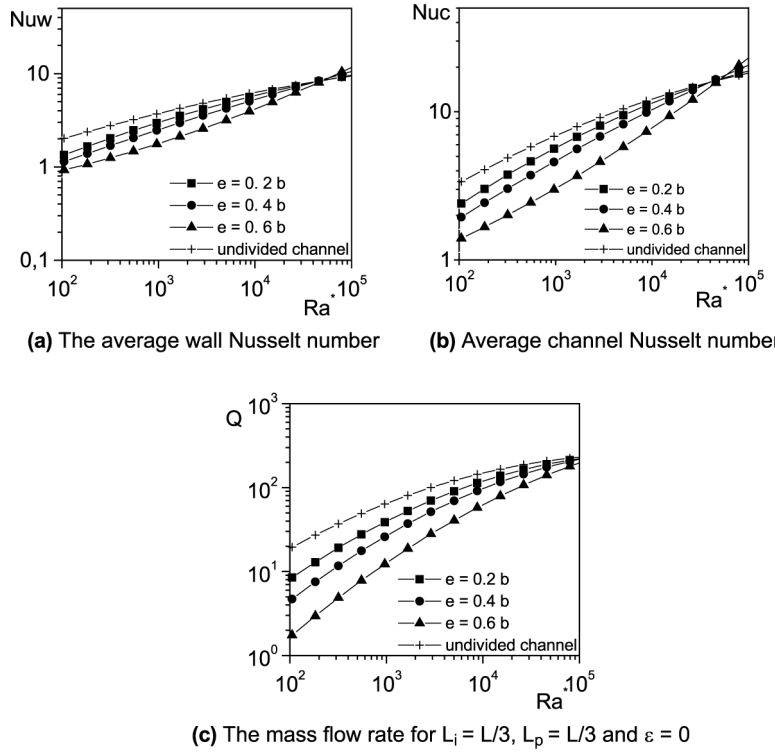

Figure 11.
Effect of the plate width

channel (Q). Within the investigated parameter ranges, the following conclusions can be drawn:

- The radiation exchange plays a very important role on the paces of the isotherms, especially at high Rayleigh numbers ($Ra^* \geq 1{,}600$), by generating two small channels between the vertical surfaces of the plate and the channel walls.
- The radiation exchange increases considerably the average wall Nusselt number (Nu_w), whereas its influence on the average Nusselt number of the channel (Nu_c) and the mass flow rate (Q) is less important.
- In the pure natural convection case ($\varepsilon = 0$), the location of the plate has no significant effect on Nu_w, Nu_c and Q, whereas it affects considerably the structures of streamlines and isotherms in presence of radiation exchange, particularly at high Ra^*. In this last case ($\varepsilon = 1$), the best position of the plate was found close to the inlet of the channel.
- The increase of both length and width of the plate produces a decrease in Nu_w, Nu_c and Q. In the pure natural convection case, these numbers are lower than those obtained in the case of an undivided channel (with the same geometry and the same boundary conditions); whereas the radiation exchange increases these numbers and reduces the difference (observed at $\varepsilon = 0$) between them.

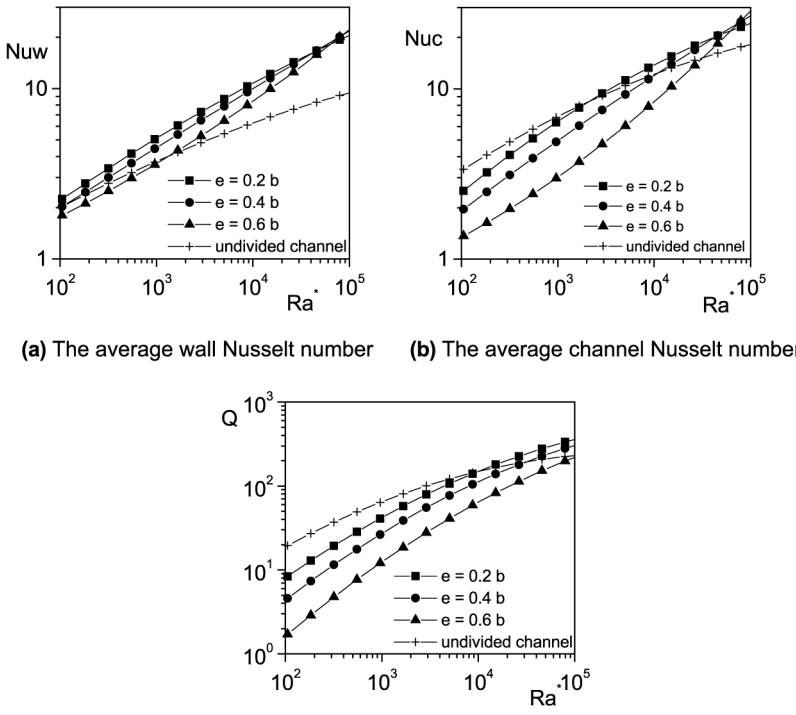

(a) The average wall Nusselt number **(b)** The average channel Nusselt number

(c) The mass flow rate for $L_i = L/3$, $L_p = L/3$ and $\varepsilon = 1$

Figure 12.
Effect of the plate width

References

Aihara, T. (1973), "Effects of inlet boundary-conditions on numerical solutions of free convection between vertical parallel plates", *Report, Institute of High Speed Mechanics*, Vol. 28, No. 256, Tohoku University, Sendai, pp. 1-27.

Andreozzi, A. and Manca, O. (2001), "Thermal and fluid dynamic behaviour of symmetrically heated vertical channels with auxiliary plate", *International Journal of Heat and Fluid Flow*, Vol. 22, pp. 424-32.

Andreozzi, A., Manca, O. and Naso, V. (2002), "Natural convection in vertical channels with an auxiliary plate", *International Journal of Numerical Methods for Heat & Fluid Flow*, Vol. 12 No. 6, pp. 716-34.

Aung, W., Fletcher, L.S. and Sernas, V. (1972), "Developing laminar free convection between vertical flat plates with asymmetric heating", *International Journal of Heat & Mass Transfer*, Vol. 15, pp. 2293-308.

Bodoia, J.R. and Osterle, J.F. (1962), "The development of free convection between heated vertical plates", *Journal of Heat Transfer*, Vol. 84, pp. 40-4.

Carpenter, J.R., Briggs, D.G. and Sernas, V. (1976), "Combined radiation and developing laminar free convection between vertical flat plates with asymmetric heating", *Journal of Heat Transfer*, February, pp. 95-100.

Cheng, X. and Müller, U. (1998), "Turbulent natural convection coupled with thermal radiation in large vertical channels with asymmetric heating", *International Journal of Heat & Mass Transfer*, Vol. 41 No. 12, pp. 1681-92.

Cruchaga, M. and Celentano, D. (2003), "Modelling natural and mixed convection in obstructed channels", *International Journal of Numerical Methods for Heat & Fluid Flow*, Vol. 13 No. 1, pp. 57-85.

Desrayaud, G. and Fichera, A. (2002), "Laminar natural convection in a vertical isothermal channel with symmetric surface-mounted rectangular ribs", *International Journal of Heat & Fluid Flow*, Vol. 23, pp. 519-29.

Elenbaas, W. (1942), "Heat dissipation of parallel plates by free convections", *Physica*, Vol. 9, pp. 1-28.

Habchi, S. and Acharia, S. (1986), "Laminar mixed convection in a partially blocked, vertical channel", *International Journal of Heat & Mass Transfer*, Vol. 29, pp. 1711-22.

Kettleborough, C.F. (1972), "Transient laminar free convection between heated vertical plates including entrance effects", *International Journal of Heat & Mass Transfer*, Vol. 15, pp. 883-96.

Mezrhab, A. and Bchir, L. (1999), "Radiation-natural convection interactions in partitioned cavities", *International Journal of Numerical Methods for Heat & Fluid Flow*, Vol. 9 No. 2, pp. 186-203.

Moutsoglou, A., Rhee, J.H. and Won, J.H. (1992), "Natural convection-radiation cooling of a vented channel", *International Journal of Heat & Mass Transfer*, Vol. 35 No. 11, pp. 2855-63.

Nakamura, H., Yutaka, A. and Naitou, T. (1982), "Heat transfer by free convection between two parallel flat plates", *Numerical Heat Transfer*, Vol. 5, pp. 95-106.

Naylor, D. and Tarasuk, J. (1993a), "Natural convective heat transfer in a divided vertical channel: Part 1 – Numerical study", *ASME Journal of Heat Transfer*, Vol. 115, pp. 377-87.

Naylor, D. and Tarasuk, J. (1993b), "Natural convective heat transfer in a divided vertical channel: Part II. Experimental study", *ASME Journal of Heat Transfer*, Vol. 115, pp. 388-94.

Naylor, D., Floryan, J.M. and Tarasuk, J.D. (1991), "A numerical study of developing free convection between isothermal vertical plates", *ASME Journal of Heat Transfer*, Vol. 113, pp. 620-6.

Tanda, J. (1997), "Natural convection heat transfer in vertical channels with and without transverse square ribs", *International Journal of Heat & Mass Transfer*, Vol. 40 No. 9, pp. 2173-85.

Teertstra, P., Culham, J.R., Yovanovich, M.M. and Lee, S. (1995), "Analytical model for simulating the thermal behavior of microelectronic systems", *Advances in Electronic packaging ASME*, EEP – Vol. 10-2.

Zhong, Z.Y., Yang, K.T. and Lloyd, J.R. (1985), "Variable property effects in laminar natural convection in a square enclosure", *Journal of Heat Transfer*, Vol. 17, pp. 133-8.

Corresponding author
A. Mezrhab can be contacted at mezrhab@sciences.univ-oujda.ac.ma